Time-domain radiative properties of a single subwavelength aperture surrounded by an exit side surface corrugation

Amit Agrawal and Ajay Nahata

Department of Electrical and Computer Engineering, University of Utah, Salt Lake City, UT 84112
agrawal@eng.utah.edu, nahata@ece.utah.edu

Abstract: Using experiment and simulation, we describe the radiative properties of a single subwavelength aperture surrounded by concentric annular grooves on the exit surface using terahertz (THz) time-domain techniques. The approach allows for the unique determination of the contribution from each exit surface annular groove to the radiated THz temporal waveform. Based on a simple model, we discuss why the grooves on the exit surface necessarily enhance the time-integrated THz power radiated from the metal structure relative to an equivalent bare aperture. Each exit side groove is shown to produce a time-delayed replica of the total THz pulse that is evanescently coupled through the subwavelength aperture. These replicas are coherently superposed on each other and temporally shifted from one another in accordance with the spatial distance between the grooves. The use of patterns incorporating double-sided surface corrugation therefore allows for greater flexibility in generating complex temporal THz pulse shapes.

OCIS codes: (050.1220) Apertures; (240.6680) Surface plasmons; (240.6690) Surface waves; (260.3090) Far-infrared

References and links

1. H. Bethe, "Theory of diffraction by small holes," Phys. Rev. **66**, 163-182 (1944).
2. C. J. Bouwkamp, "Diffraction theory," Rep. Prog. Phys. **17**, 35-100 (1954).
3. H. J. Lezec, A. Degiron, E. Devaux, R. A. Linke, F. Martin-Moreno, L. J. Garcia-Vidal, and T.W. Ebbesen, "Beaming light from a subwavelength aperture," Science **297**, 220-222 (2002).
4. F. I. Baida, D. Van Labeke, and B. Guizal, "Enhanced confined light transmission by single subwavelength apertures in metallic films, Appl. Opt. 42, 6811-6815 (2003).
5. L. Martin-Moreno, F. J. Garcıa-Vidal, H. J. Lezec, A. Degiron, and T.W. Ebbesen, "Theory of highly directional emission from a single subwavelength aperture surrounded by surface corrugations," Phys. Rev. Lett. **90**, 167401(2003).
6. F. J. Garcıa-Vidal, L. Martin-Moreno, H. J. Lezec and T. W. Ebbesen, "Focusing light with a single subwavelength aperture flanked by surface corrugations," Appl. Phys. Lett. **83**, 4500-4502 (2003).
7. F. J. Garcıa-Vidal, H. J. Lezec, T. W. Ebbesen, and L. Martin-Moreno, "Multiple paths to enhance optical transmission through a single subwavelength slit," Phys. Rev. Lett. **90**, 213901/1-4 (2003).
8. M. J. Lockyear, A. P. Hibbins, J. R. Sambles, C. R. Lawrence, "Surface-topography-induced enhanced transmission and directivity of microwave radiation through a subwavelength circular metal aperture," Appl. Phys. Lett. **84**, 2040-2042 (2004).
9. M. J. Lockyear, A. P. Hibbins, J. R. Sambles, and C. R. Lawrence, "Enhanced microwave transmission through a single subwavelength aperture surrounded by concentric grooves," J. Opt. A: Pure Appl. Opt. **7**, S152-S158 (2005).
10. T. Thio, K. M. Pellerin, R. A. Linke, H. J. Lezec, and T. W. Ebbesen, "Enhanced light transmission through a single subwavelength aperture," Opt. Lett. **26**, 1972-1974 (2001).
11. T. Thio, H. J. Lezec, T. W. Ebbesen, K. M. Pellerin, G. D. Lewen, A. Nahata, R. A. Linke, "Giant optical transmission of sub-wavelength apertures: physics and applications," Nanotechnology **13**, 429-432 (2002).
12. A. Agrawal, H. Cao, and A. Nahata, "Excitation and scattering of surface plasmon-polaritons on structured metal films and their application to pulse shaping and enhanced transmission," New J. Phys. **7**, 249 (2005), http://www.iop.org/EJ/abstract/1367-2630/7/1/249.
13. D. Grischkowsky, in *Frontiers in Nonlinear Optics*, H. Walther, N. Koroteev, and M. O. Scully, eds. (Institute of Physics Publishing, Philadelphia, 1992) and references therein.

#9992 - $15.00 USD Received 16 December 2005; received 27 January 2006; accepted 20 February 2006

14. H. Cao, A. Agrawal, and A. Nahata, "Controlling the transmission resonance lineshape of a single subwavelength aperture," Opt. Express **13,** 763-769 (2005), http://www.opticsexpress.org/abstract.cfm?URI=OPEX-13-3-763.
15. A. Agrawal, H. Cao, and A. Nahata, "Time-domain analysis of enhanced transmission through a single subwavelength aperture," Opt. Express **13,** 3535-3542 (2005), http://www.opticsexpress.org/abstract.cfm?URI=OPEX-13-9-3535.

1. Introduction

Radiation and diffraction play a fundamental role within the general field of electromagnetics. An important example that relies on these two processes is that of light exiting an aperture. In the limit where the aperture is small compared to the wavelength of the radiation, it can be modeled as a point source and, thus, the exiting radiation is diffracted into the half sphere and the corresponding spatial distribution can be modeled by considering the radiation from a dipole [1, 2]. Recently, Lezec et al. demonstrated that when periodic surface corrugations surround the subwavelength aperture on the exit surface, the light radiated from the metal-dielectric interface could be highly directional [3]. They discuss a simple far-field model that qualitatively confirms their observations. Within this model, light is radiated not only from the aperture, but also from the center of each of the periodically spaced grooves. They further assume that the phase relationship between the light radiated from each groove and the aperture corresponds directly to the distance between these two features. While the model is reasonable and generally agrees with their experimental observations, there has been no experimental verification of their assumptions to our knowledge.

The focus of much of the subsequent theoretical and experimental studies has been on further examining the role that the grooves on the exit surface of the metal film play in determining the spatial distribution of the radiated light [3-9]. With appropriate corrugation pattern on the output metal surface, it has been shown theoretically that the structure can focus the radiated electromagnetic field [6]. Within many of these studies, there has also been discussion concerning the role these exit surface grooves play in the transmission enhancement process [5-9]. These studies, both theoretical and experimental in nature, suggest that the exit side structures determine primarily the spatial distribution of the radiated light and play a weak role, at best, in the transmission enhancement process.

In this submission, we measure the time-domain radiative properties of a single subwavelength aperture surrounded by concentric annular periodically spaced grooves (bullseye structures [10, 11]) on the exit surface of the metal film. Using conventional terahertz (THz) time-domain spectroscopy, we can uniquely determine the contribution of each exit surface annular groove to the radiated THz temporal waveform and give a simple model to describe the radiation process. A combination of experimental data and simulation are used to demonstrate that the each exit side groove produces a time-delayed replica of the total THz pulse that is evanescently coupled through the subwavelength aperture to the exit surface. These replicas are coherently superposed on each other, though temporally shifted from one another in accordance with the spatial distance between the grooves. We have previously shown that complex THz pulse shapes may be generated by varying the groove spacing and controlling the cross-section of each individual groove on the input metal surface [12]. The ability to structure both metal surfaces independently should allow for far greater flexibility in generating arbitrary THz pulse shapes. As we discuss below, this is not equivalent to creating the two separate patterns overlaid on the input surface. Finally, we discuss why the grooves on the exit surface necessarily enhance the time-integrated THz power radiated from the metal structure relative to an equivalent structure with no exit surface corrugation.

#9992 - $15.00 USD Received 16 December 2005; received 27 January 2006; accepted 20 February 2006

2. Experimental details

The experimental studies were performed on bullseye structures that consisted of a single 490 μm diameter central circular aperture surrounded by a variable number of concentric annular rectangular cross-section grooves on one or both metal surfaces. We fabricated several sets of these structures on 175 μm thick free-standing stainless steel metal foils using conventional chemical etching techniques. The first set of samples consisted of four bullseye patterns with two, four and six periodically spaced annular grooves surrounding the aperture. The annular groove depth and width and depth were 100 μm and 500 μm, respectively, with a periodic spacing of 0.8 mm. The samples could be reversed in the experimental setup to compare the time-domain properties of having annular grooves only on the input surface versus having them only on the exit surface. For reference purposes, we fabricated 490 μm diameter bare apertures on metal foils of identical thickness. The second set of samples contained bullseye patterns with one or more annular groove on both the entrance and exit side of the metal foil. For this second set of samples, the grooves had a depth and width of 75 μm and 500 microns respectively. In this latter set of samples, the minimum metal thickness at locations where the grooves on the two metal surfaces spatially overlapped was ~25 μm. This value is much greater than the skin depth for typical metals at frequencies below 1 THz (<1 μm).

We used a conventional time-domain THz spectroscopy setup [13] to characterize the bullseye structures and bare apertures. Details of the experimental setup and the advantageous properties of this approach for the present purposes have been discussed previously [14] and, therefore, are only briefly presented here. Photoconductive devices were used for both emission and coherent detection. An off-axis paraboloidal mirror was used to collect and collimate the THz radiation from the emitter to the samples. In all cases, the THz beam was normally incident on the bullseye patterns. Coherent THz pulses radiated from the exit surface of the metal foil were focused onto the photoconductive detector. Because of the experimental geometry, however, the detection efficiency was progressively reduced with increasing distance between the aperture and the radiating element (i.e. the annular grooves).

3. Time-domain radiative properties of grooves

Figure 1(a) shows schematic cross-sectional views of bullseye structures containing zero, two, four, and six periodically spaced annular grooves surrounding the subwavelength aperture on the exit surface only. As noted above, the THz radiation is incident on the plane (unstructured) metal side of the foil. Figure 1(b) shows the corresponding measured temporal THz waveforms. As we have previously shown, the measured waveform for the reference bare aperture is characterized by a single bipolar waveform, while the waveforms for bullseye structures consist not only of this initial bipolar waveform, but also a damped oscillatory signal [12, 14, 15]. For the waveforms associated with the four bullseye structures in Fig. 1(b), the initial bipolar pulse is nearly identical in shape and magnitude to that for the bare aperture. Furthermore, there is a one-to-one correspondence between the number of grooves and the number of oscillations following the initial bipolar pulse component.

In order to further explain the data, consider the schematic drawing in Fig. 2. In both diagrams, the input metal face is uncorrugated, since this reflects the experimental conditions used in the initial experimental results mentioned above. The discussion that follows may be generalized for metal films that are corrugated on both surfaces. In Fig. 2, radiation is normally incident on the metal foils from above. The total time-varying electric field at the input face of the aperture, arising from the directly incident THz beam (or via interaction with the metal structuring on the input surface for bullseye geometries with double sided corrugation), evanescently tunnels through the subwavelength aperture. A fraction of this field directly radiates into the far-field from the aperture, while the remainder couples to propagating surface waves on the exit surface. In the absence of any exit side surface corrugation, depicted in Fig. 2(a), only the THz waveform radiated from the aperture would be observed. In the case of a bare aperture, this would correspond to a single bipolar waveform, which is consistent with our observations. With the inclusion of an exit side

#9992 - $15.00 USD Received 16 December 2005; received 27 January 2006; accepted 20 February 2006

surface corrugation, each groove would radiate a fraction of the propagating surface wave in the forward direction towards the THz detector. In this case, the observed time-domain waveform would consist not only of the initial bipolar waveform, but also a superposition of coherent time-delayed oscillations, as depicted in Fig. 2(b). Therefore, we would expect a one-to-one correspondence between the number of grooves and the number of observed oscillations after the initial bipolar pulse. Again, this is consistent with our experimental observations.

Returning now to the experimental results of Fig. 1(b), it is apparent that there are a number of low amplitude oscillations following the primary oscillations, particularly for the 4 an 6 annular groove bullseye structures. These are believed to be caused by in-plane scattering of the surface waves from adjacent grooves. The decrease in the amplitude of successive oscillations in the time-domain waveforms is attributed to the reduced amplitude of the surface wave pulses as they move away from the aperture, because of in-plane and out-of-plane scattering from preceding grooves, as well as a progressive reduction in the detection efficiency as the distance between the radiation point and the aperture increases.

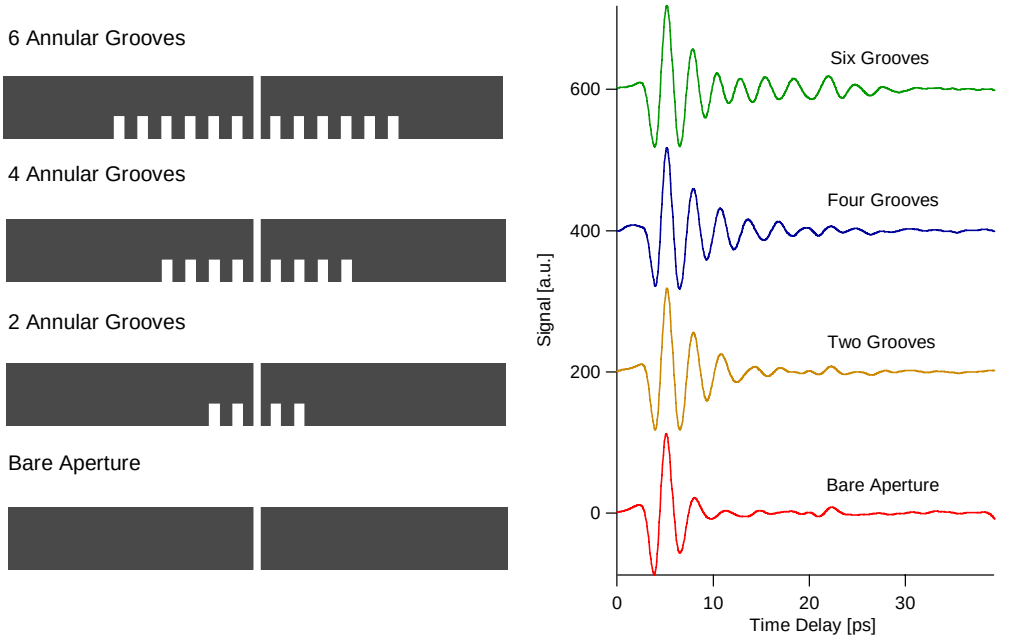

(a) (b)

Fig. 1. Transmitted time-domain waveforms through bullseye structures consisting of periodic multiple annular grooves on the exit surface. In all cases, broadband THz radiation is incident on the structures from above (a) Cross-sectional line diagrams of the structures containing zero, two, four and six periodically spaced concentric annular grooves (b) Experimentally observed time-domain waveforms for the structures shown in part (a). The temporal waveforms have been offset from the origin for clarity. The number of oscillations, after the initial bipolar waveform, matches the number of annular grooves on the exit side. The small oscillation present at ~22 ps in all of the waveforms is caused by a reflection with the experimental system.

While the correspondence between the number of oscillations in the time-domain waveforms in Fig. 1(b) and the number of annular grooves strongly suggests the validity of the diagram in Fig. 2(b), it is necessary to further examine the specific timing of each oscillation. In order to accomplish this, we use the bullseye structure containing four annular grooves shown in Fig. 1(a). Figure 3 shows the transmitted THz time-domain waveforms measured with the annular grooves on the input surface versus on the output surface. We have

#9992 - $15.00 USD Received 16 December 2005; received 27 January 2006; accepted 20 February 2006

previously shown that when the annular grooves are on the input surface, each annular groove acts to couple in a large fraction of the incident THz pulse and that the time delay between an oscillation and the initial bipolar contribution in the observed THz waveform corresponds directly to the spacing between the associated groove and the aperture [15]. When the annular grooves are on the exit surface, the timing of the oscillations does not change, demonstrating clearly that it is the center-to-center spacing between surface features in the metal foil that lead to the relevant time delays in the transmitted THz waveforms. It is worth pointing out that the amplitudes of identically timed oscillations obtained with these two sample orientations are not expected to be the same. For grooves on the input surface, the oscillation amplitudes are determined, in part, by the spatial properties of the incident THz beam. For the grooves on the exit surface, the oscillation amplitudes are determined, in part, by the collection and detection properties of the experimental system.

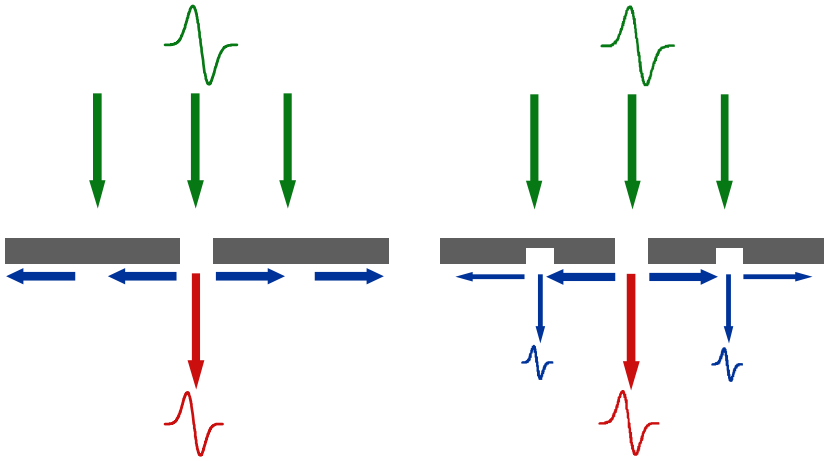

Fig. 2. Schematic diagram showing the transmission mechanism through (a) a bare subwavelength aperture, (b) a subwavelength aperture surrounded by grooves on the exit side. The component shown by the red arrow corresponds to the waveform component radiated by the subwavelength aperture. The component shown by the blue arrow corresponds to the bound surface modes coupled to the metal-dielectric interface on the exit side. These bound modes are partially radiated by scattering from the grooves on the exit side. This latter component is temporally delayed with respect to the initial bipolar waveform.

Based on the simple radiative model shown in Fig. 2 and the ensuing discussion, we now describe how the time-domain properties of bullseye structures with double-sided surface corrugation may be ascertained from nominally equivalent structures with only an input surface corrugation. Such a capability is important not only in the understanding of the operational properties of these structures, but also may be used to create more complex THz pulse shaping capabilities. As mentioned above, an electromagnetic field associated with the interaction of freely propagating radiation and the structured surface of the input metal surface evanescently tunnels through the subwavelength aperture. A fraction of this field radiates from the aperture, while the remainder propagates away from the aperture in the form of a surface plasmon-polariton wave bound to the metal-dielectric interface. The surface propagating wave nominally has the same temporal properties as the electromagnetic field radiated from the aperture. As this surface wave interacts with surface features, annular grooves in our case, a portion is radiated in the same forward direction as the field radiated from the aperture. This latter radiated field is time-delayed in direct relation to the propagation distance from the aperture. Therefore, the observed far-field THz time-domain waveform, E_{tot}, from a structure that is corrugated on the exit surface may be written as

#9992 - $15.00 USD Received 16 December 2005; received 27 January 2006; accepted 20 February 2006

$$E_{tot}(t) = \sum_{n} c_n \, E_{ap}(t - T_n), \qquad (1)$$

where $E_{ap}(t)$ is the observed far-field THz temporal waveform radiated only by the subwavelength aperture, n is the groove number with the condition that n = 0 corresponds to the aperture, T_n is the delay associated with groove number n ($T_0 = 0$), and c_n is a constant that accounts for the radiation of surface structure n, as well as the collection and detection efficiency from that structure ($c_0 = 1$). Therefore c_n depends not only on the properties of the grooves, but also on the details of the detection system.

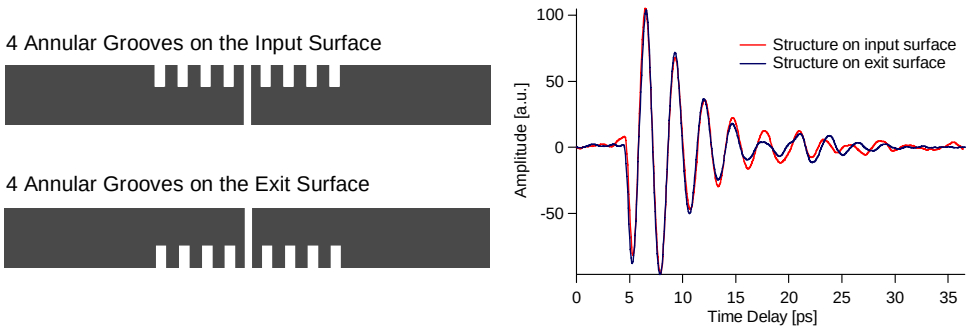

(a) (b)

Fig. 3. (a) Cross-sectional line diagrams of bullseye structures with four annular grooves on the entrance and the exit surface (b) Transmitted time-domain waveforms through the structures shown in part (a). The temporal overlap of the contributions from individual grooves for the two sample orientations demonstrates clearly that the center-to-center spacing between features on the exit surface of the metal foil leads to the relevant time delays in the transmitted THz waveforms.

In order to demonstrate the validity of this time-domain model, we begin by considering a simple example using two specific structures examined in detail above: a bare aperture and a bullseye structure with four annular grooves on the exit surface. Therefore, in this initial example, the input surface is not corrugated. The temporal waveform associated with the bare aperture is a single bipolar waveform, which we define as $E_{ap}(t)$, while the waveform for the bullseye structure corresponds to $E_{tot}(t)$. According to Eq. (1), the temporal waveform for the bullseye structure should be simply the coherent superposition of an initial bipolar waveform and four scaled time-delayed copies. Figure 4 shows the measured waveform for the four groove bullseye structure and simulation results using Eq. (1), with $c_0 = 1$, T_0=0, $c_1 = 0.42$, T_1=2.8 ps, $c_2 = 0.32$, T_2=5.6 ps, $c_3 = 0.23$, T_3=8.4, and $c_4 = 0.11$, T_4=11.2 ps. The agreement between experiment and simulation is excellent for the initial bipolar waveform and the subsequent four oscillations. Beyond that point, the agreement is not as good because the temporal waveform associated with the bare aperture does not include any secondary oscillations arising from in-plane scattering that are present in the four groove bullseye structure.

More generally, this basic approach may be applied to structures in which both metal surfaces are corrugated. Figure 5(a) shows schematic cross-sectional diagrams of a bullseye pattern with four annular grooves on the input surface and a second bullseye pattern with four annular grooves on the input surface and a single annular groove on the exit surface at the same spatial position as the second input groove. The measured THz time-domain waveforms for these samples are shown in Fig. 5(b). We define the waveform of the upper structure as $E_{ap}(t)$, while the waveform for the lower structure corresponds to $E_{tot}(t)$. Figure 5(c) show the experimental data for the double-sided bullseye structure, again, and the corresponding

#9992 - $15.00 USD Received 16 December 2005; received 27 January 2006; accepted 20 February 2006

simulation. Here, we assumed that $c_0 = 1$, $T_0=0$, $c_1 = 0.42$, $T_1=2.8$ ps. It is important to point out that the value of c_1 corresponding to a 2.8 ps time delay is exactly the same as used to obtain Fig. 4. In general, we have found that the value of the constants (c_n) remain constant for specific T_n values from sample to sample.

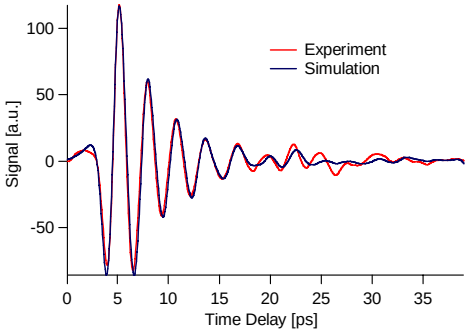

Fig. 4. Comparison between experiment and theory for a four groove bullseye structure. The red trace corresponds to the transmitted THz waveform obtained for the bullseye structure with the grooves on the exit surface. The blue trace corresponds to results from a simulation obtain by using Eq. (1) and assuming $E_{ap}(t)$ corresponds to the temporal waveform for a bare aperture.

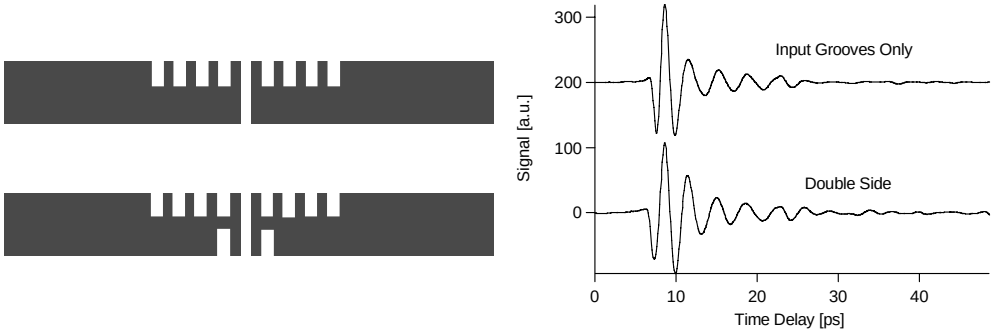

#9992 - $15.00 USD Received 16 December 2005; received 27 January 2006; accepted 20 February 2006

(a) (b)

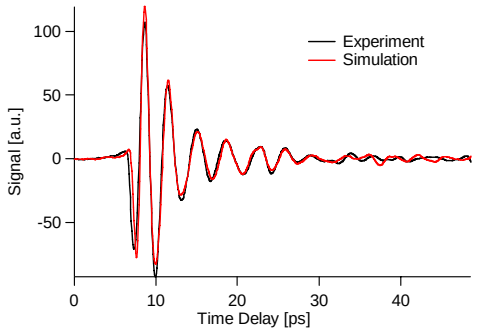

(c)

Fig. 5. Comparison between experiment and theory for a bullseye structure with double sided corrugation. (a) Schematic cross-sectional views of bullseye structures with annular grooves on one or both surfaces (b) The transmitted time-domain waveforms for the structures shown in part (a). (c) The black trace corresponds to the experimentally observed time-domain waveform for the bullseye structure with double-sided corrugation. The red trace corresponds to results from a simulation obtain by using Eq. (1) and assuming Eap(t) is given by the temporal waveform for a bullseye structure corrugated on only the input surface.

As we noted in the introduction, the ability to corrugate the two metal surfaces should allow for far greater flexibility in pulse shaping applications. It is important to note that such double-sided corrugation is not equivalent to overlaying both surface patterns on one surface only. In order to clarify this point, consider the experimental results shown in Fig. 5. The double-sided structure contains four periodically spaced concentric annular grooves, while the exit surface contains only one annular groove. This exit surface groove is in the same location as the first groove, immediately adjacent to the aperture, on the input face. If both patterns were overlaid on the input surface, for example, the input surface would look similar to the initial four groove input surface, with the first groove being twice as deep. The resulting waveform would look similar to the waveform obtained with the four uniform groove input surface (i.e. four oscillations after the initial bipolar pulse component), while the double-sided structure should contain five oscillations after the initial bipolar pulse component. This is exactly what we observe experimentally, as shown in Fig. 5.

Finally, we can now address the role that a surface corrugation on the exit surface surrounding a subwavelength aperture plays in the transmission enhancement process. As we have shown, a well-defined fraction of the electromagnetic field that evanescently tunnels through the subwavelength aperture is directly radiated into the far-field. This fraction does not depend upon the presence of the exit side surface corrugation, as demonstrated by the fact that the initial bipolar waveform component is essentially identical for all of the fabricated samples. When no exit side surface corrugation is present (i.e. a bare aperture), the surface waves remain bound to the metal-dielectric interface and propagate until completely attenuated. This attenuation is caused by the finite conductivity of the metal. With the presence of a surface corrugation (i.e. annular grooves in our case), a portion of the propagating surface wave is radiated in the same forward direction as that radiated by the aperture. Therefore, an exit side surface corrugation not only alters the spatial distribution of the transmitted radiation, but also necessarily enhances the total time-integrated power radiated from such structures.

3. Conclusion

In this submission, we have measured the time-domain radiative properties of a single subwavelength aperture surrounded by concentric annular periodically spaced grooves (bullseye structures) on the exit surface of the metal film. Using conventional THz time-domain spectroscopy, the contribution of each exit surface annular groove to the radiated THz

#9992 - $15.00 USD Received 16 December 2005; received 27 January 2006; accepted 20 February 2006

temporal waveform may be uniquely determined. Each exit side groove is shown to produce a time-delayed replica of the total THz pulse that is evanescently coupled through the subwavelength aperture. The transmitted THz waveform, therefore, contains replicas that are coherently superposed and temporally shifted from one another in accordance with the spatial distance between the grooves. These observations are well described by a model of the radiation process. Based on this model, we discuss why the grooves on the exit surface necessarily enhance the total time-integrated THz power radiated from the metal structure relative to an equivalent structure with an uncorrugated exit surface. We have previously shown that complex THz pulse shapes may be generated by varying the groove spacing and controlling the cross-section of each individual groove on the input metal surface [12, 14, 15]. The ability to structure both metal surfaces independently should allow for far greater flexibility in generating arbitrary THz pulse shapes. The results of the present manuscript, along with recent prior work [12, 14, 15], yield a nearly complete time-domain description of the enhanced transmission process through these structures.

#9992 - $15.00 USD Received 16 December 2005; received 27 January 2006; accepted 20 February 2006